Alagille syndrome is caused by mutations in human *Jagged1*, which encodes a ligand for Notch1

Linheng Li[1,6], Ian D. Krantz[2], Yu Deng[3,6], Anna Genin[2], Amy B. Banta[1,6], Colin C. Collins[4], Ming Qi[5], Barbara J. Trask[6], Wen Lin Kuo[7], Joanne Cochran[4], Teresa Costa[8], Mary Ella M. Pierpont[9], Elizabeth B. Rand[10], David A. Piccoli[10], Leroy Hood[1,6] & Nancy B. Spinner[2]

Alagille syndrome is an autosomal dominant disorder characterized by abnormal development of liver, heart, skeleton, eye, face and, less frequently, kidney. Analyses of many patients with cytogenetic deletions or rearrangements have mapped the gene to chromosome 20p12, although deletions are found in a relatively small proportion of patients (< 7%). We have mapped the human *Jagged1* gene (*JAG1*), encoding a ligand for the developmentally important Notch transmembrane receptor, to the Alagille syndrome critical region within 20p12. The Notch intercellular signalling pathway has been shown to mediate cell fate decisions during development in invertebrates and vertebrates. We demonstrate four distinct coding mutations in *JAG1* from four Alagille syndrome families, providing evidence that it is the causal gene for Alagille syndrome. All four mutations lie within conserved regions of the gene and cause translational frameshifts, resulting in gross alterations of the protein product. Patients with cytogenetically detectable deletions including *JAG1* have Alagille syndrome, supporting the hypothesis that haploinsufficiency for this gene is one of the mechanisms causing the Alagille syndrome phenotype.

Alagille syndrome (AGS, OMIM#118450) is an autosomal dominant developmental disorder that affects structures in the liver, heart, skeleton, eye, face, kidney and other organs[1,2]. It occurs with a minimal estimated frequency of 1:70,000 live births (when ascertained by the presence of neonatal jaundice[3]), with the true incidence most likely being higher. The syndrome has traditionally been defined by a paucity of intrahepatic bile ducts, in association with five main clinical abnormalities (cholestasis, cardiac disease, skeletal abnormalities, ocular abnormalities and a characteristic facial phenotype) (Fig. 1). Cholestasis is a direct consequence of the paucity of bile ducts. Cardiac anomalies most commonly involve the peripheral and main pulmonary arteries as well as the pulmonary valves. These lesions may range from clinically insignificant peripheral pulmonic stenosis to complex defects such as tetralogy of Fallot. The most common skeletal anomalies are 'butterfly' or hemivertebrae, resulting from clefting abnormalities of the vertebral bodies. Ocular lesions include anterior chamber defects, most commonly posterior embryotoxon (a benign defect), and retinal pigmentary abnormalities. Facies have been described as triangular, consisting of a prominent forehead, deep-set eyes, hypertelorism, long, straight nose with flattened tip, short philtrum, flat midface and a triangular chin. Renal and neurodevelopmental abnormalities occur less frequently[4]. Fifteen percent of patients will require liver transplantation and 7–10% of patients have severe congenital heart disease, most often tetralogy of Fallot[5]. Diagnosis in a proband is made if bile duct paucity is accompanied by three of the five main clinical criteria[1]. It has been suggested that family members of a proband are 'affected' if they express any of the five main clinical features (variable expressivity)[6,7].

Many patients have deletions of 20p11-12, suggesting that the disease gene lies in this region[4,8,9,10]. The initial association of deletions with a multisystem disorder led to the hypothesis that this may be a contiguous gene deletion syndrome. However, the frequency of observable deletions is low, suggesting that this disorder may result from mutations in a single gene with pleiotropic effects[4,10,11]. We previously refined the localization of the Alagille syndrome critical region to a 1.5-Mb segment based on analysis of the shortest region of overlap of the deletions in a series of patients[4].

We have mapped the human homologue of the rat *Jagged1* gene (*JAG1*) to chromosome 20p12[12]. Jagged is a ligand for the transmembrane receptor Notch. The Notch family of proteins was originally identified in *Drosophila* and has been shown to play an essential role in cell fate determination in numerous cell lineages[13–15]. The Notch family is highly conserved from invertebrate to vertebrate[16–22], and the Notch proteins have been shown to be involved in the regulation of development of a variety of mammalian tissues[23–25]. Four Notch family members have thus far been identified in humans[15,27,28] (Li, L. *et al.*, manuscript submitted).

[1]*Stowers Institute for Medical Research,* [6]*Department of Molecular Biotechnology, University of Washington, Seattle, Washington 98195, USA.* [2]*Division of Human Genetics,* [10]*Division of Gastroenterology and Nutrition, The Children's Hospital of Philadelphia, University of Pennsylvania School of Medicine, 324 S 34th Street, Philadelphia, Pennsylvania 19104, USA.* [3]*Institute of Genetics, Fudan University, Shanghai, 200433, China.* [4]*Resource for Molecular Cytogenetics, Life Sciences Division, Lawrence Berkeley National Laboratory, Berkeley, California 94720, USA.* [5]*Division of Medical Genetics, Departments of Medicine & Pathology, University of Washington, Seattle, WA 98195, USA.* [7]*University of California San Francisco Cancer Center, Cancer Genetics Program, San Francisco California 941413, USA.* [8]*The Hospital for Sick Children, Department of Genetics, 555 University Avenue Toronto, Ontario M5G 1X8, Canada.* [9]*Department of Pediatrics and Institute of Human Genetics, University of Minnesota, Minneapolis MN, USA. Correspondence should be addressed to N.B.S. (spinner@mail.med.upenn.edu) or L.H. (lee@nirvana.MBT.Washington.edu)*

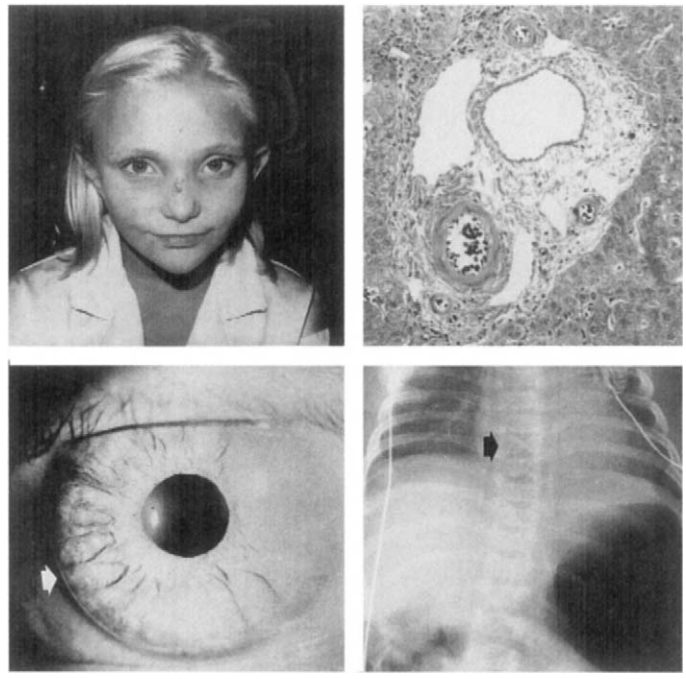

Fig. 1 Clinical features in Alagille syndrome. ***a,*** Facial features in an affected child. Note the triangular face, prominent forehead, deep-set eyes, pointed chin. ***b,*** Large portal tract with minimal fibrosis seen on a liver biopsy. Multiple branches of the hepatic artery and portal vein are present, without any accompanying bile ducts. ***c,*** Posterior embryotoxon (arrow marks the prominent Schwalbe's line). ***d,*** Butterfly vertebra due to abnormal clefting of the vertebral bodies.

Several Notch ligands are known in *Drosophila* and vertebrates (Fig. 2). The Delta and Serrate proteins were identified as ligands for the *Drosophila* Notch receptor[29]. *Jagged* was initially identified in rat and exhibits significant similarity to the *Drosophila Serrate* gene[18] (Fig. 2). Like the Delta and Serrate proteins, the rat Jagged1 (rJagged1) protein contains a highly conserved DSL domain (so named because it is conserved in Delta, Serrate and Lag-2, the ligand for the *C. elegans* Notch homologue[31]), 16 epidermal growth factor (EGF)–like repeats, and a cysteine-rich region (CR). Both the EGF-like and the DSL domains, and probably the CR domain, are important for ligand-receptor interaction[12,31,32]. The rJagged1 protein was shown to be a ligand for the Notch1 receptor because of its ability to activate the rat Notch1 receptor in myoblasts[30]. A second rat Jagged protein (rJagged2) with 73% identity to rJagged1 has also been identified[34]. We and others recently cloned the human homologue of *rJagged1*, *JAG1* (refs. 12,34), and we have shown that the JAG1 protein is a ligand for the Notch1 receptor[12].

In this report we present studies in which *JAG1* was tested as a candidate disease gene for the Alagille syndrome. We demonstrate the localization of *JAG1* in the Alagille syndrome critical region within 20p12. Four families were studied, and a distinct coding mutation was identified segregating with the disease phenotype in each family.

Mapping *JAG1* to the Alagille-syndrome critical region

We previously defined the Alagille syndrome critical region on chromosome 20p12 through studies of the minimal region of overlap of several patients with deletions in this region[4,35]. These studies placed the critical region between genetic markers *D20S41* and *D20S162*. A contig of YAC, P1 and BAC clones spans the critical region (Fig. 3). These clones were used to further narrow the critical region. The distal boundary of the region is defined by a P1 clone (20p1-158), containing the synaptosomal associated protein–25 gene (*Snap-25*). This clone was present in two copies in the patient with the most centromeric deletion[4]. The centromeric boundary of the region is defined by P-1 243b12, which is outside the deletion in the patient with the most distal deletion[4]. The size of this critical region is estimated to be 1.2–1.3 Mb. Two BAC clones, 49D9 and 125b1, containing *JAG1* and previously mapped to 20p12 (ref. 12), were sublocalized within the Alagille syndrome critical region. Using multiple PCR primers (249/250, 247/248) from BAC clone 49D9, on a panel of YAC, P1 and BAC clones, we mapped *JAG1* between *D20S894* and *D20S507* within the Alagille syndrome critical region (Fig. 3).

JAG1 Expression

JAG1 is expressed in various adult human tissues, including stomach, thyroid gland, spinal cord, lymph node, trachea, adrenal gland and bone marrow[12]. Further northern blot analyses revealed that *JAG1* is expressed in adult heart, placenta, lung, skeletal muscle, kidney and pancreas. We could not detect expression of *JAG1* in adult brain or liver tissue (Fig. 4*a*). Analysis of human fetal tissues shows high levels of *JAG1* in kidney (16–32 weeks) as well as in fetal lung (18-28 weeks) and lower levels in brain (20–25 weeks) and liver (16–32 weeks) (Fig. 4*b*). Expression of *JAG1* in heart, fetal liver, lung and kidney is consistent with a role for the JAG1 protein in the normal development of these tissues.

JAG1 gene structure

DNA array technology was used to determine the exon–intron boundaries of *JAG1* (Fig. 5*a*) (Shummer, M. *et al.*; manusdcript submitted). BAC clone 49D9 was fragmented by sonication. Fragments ranging in size from 1.5 to 2 kb were selected and ligated into an M13 bacteriophage vector. Individual single-stranded M13 clones were picked into 384-well microfilter plates, and 1,536 clones were arrayed onto four sets of nylon membranes. The arrays of the BAC 49D9 M13 fragments were hybridized with the full-length *JAG1* cDNA[12]. All positive M13 clones (~100 clones) were

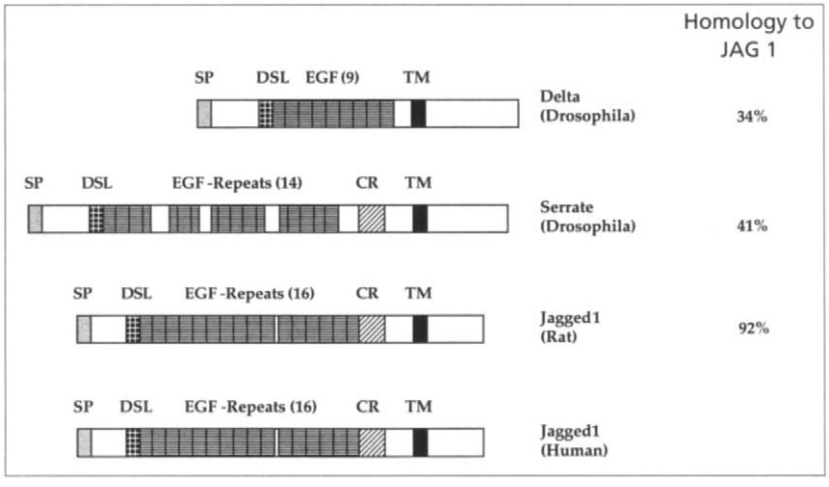

Fig. 2. Schematic diagram showing comparison of *Drosophila* Delta and Serrate, rat Jagged1 and human Jagged1 protein structures. SP, signal peptide; DSL, conserved domain shared by Delta, Serrate and Lag-2, a ligand for *C. elegans* Notch; EGF-repeats, epidermal growth factor–like repeats; CR, cysteine-rich region and TM, transmembrane region. Only Serrate and Jagged share the cysteine-rich domain.

Table 1 • The Exon/Intron Boundary Sequences of *JAG1*

Exon Number	intron/EXON...EXON/intron	*JAG1* cDNA (bp)	Exon Length(bp)
Exons 1,2	not available		
Exon 3	gttcgtgcag/AGGTCCTACA...GACACCGTTC/gtcagtatcg	801-852	52
Exon 4	ttgtctctag/AACCTGACAG...TGTAACAGAG/gtatgtgtgt	853-1107	255
Exon 5	ttttttacag/CTATTTGCCG...GTGACTGCAG/g	1108-1168	61
Exon 6	gtgtctccag/GTGCCAGTAT...TGTGACAAAG/gtatggccct	1169-1299	131
Exon 7	tttttggcag/ATCTCAATTA...TGTGAAATTG/gtaagtggtc	1300-1419	120
Exon 8	gtttttgcag/CTGAGCACGC...TGCTCTACAA/gtaagtccaa	1420-1533	114
Exon 9	tgttgaccag/ACATTGATGA...TGCCAGTTAG/gtaagaacat	1534-1647	114
Exon 10	ctcctttcag/ATGCAAATGA...TGTGACATAA/gtgagtgact	1648-1761	114
Exon 11	tatttttttag/ATATTAATGA...CTCCTGTCGG/gtatgtaaat	1762-1808	47
Exon 12	cctcttctag/GATTTGGTTA...CCTCTGTCAG/gtgagtggtg	1809-1982	174
Exon 13	atatttgcag/CTGGACATCG...CCCTGTGAAG/gtacctccct	1983-2133	151
Exon 14	tatcttctag/TGATTGACAG...TGCCATGAAA/gtaagactcc	2134-2298	165
Exon 15	tgtttcatag/ATATTAATGA...TGTGAAACCA/aagagtgtgc	2299-2412	114
Exon 16	ttgattctag/ATATTAATGA...GGCCACTCAC/gtaagtggta	2413-2526	114
Exon 17	tttcctccag/GTGACAGTCA...TGTAACATAG/gtaactttat	2527-2640	114
Exon 18	tcttttatag/CCCGAAACAG...TGTGCTCAGA/gtgagtgtcc	2641-2757	117
Exon 19	ttctttgcag/ATACCAATGA...CTCATCCCTG/gtaagtgtga	2758-2785	28
Exon 20	gctttcttag/TTACAACAGC...TGCAGAATAA/gtaaggactg	2786-2871	86
Exon 21	tttctcctag/ACATCAATGA...TGCCAGGAAG/gtatgtgtgc	2872-2985	114
Exon 22	cacctgtcag/TTTCAGGGAG...CTGCTCAAAG/gtaggacatg	2986-3095	110
Exon 23	ttttctccag/GTCTGGTGTG...GATGTCACCA/gtatgtaaca	3096-3329	234
Exon 24	atcgttttag/GGTCTTACTA...TGTGGCCATT/gtaagtataa	3330-3461	132
Exon 25	gtttttccag/TCTGCTGAAG...AACAGAACAG/gtaggtgtca	3462-3612	151
Exon 26	tgccttacag/ATTTCCTTGT...	3613-4404+	792+

picked and sequenced (Fig. 5*a*). The *JAG1* genomic and cDNA sequences were aligned, and 47 intron/exon boundaries were defined (Fig. 5*b*, Table 1). Alignment of these boundaries with the cDNA sequence revealed that we had not identified exons corresponding to the cDNA sequence from bp 414 (ATG start codon) to bp 801. The missing coding sequence is contained in two exons[36].

Identification of mutations in *JAG1*

JAG1 contains 26 exons (Fig. 5*b*) and its mRNA is 5.5 kb in size. To simplify the mutation search in Alagille syndrome patients, we began screening by heteroduplex mobility analysis (HMA)[37] on 6 RT-PCR products (from peripheral blood leukocytes) spanning the *JAG1* mRNA. HMA analysis can readily detect mutations in heterozygotes at a given locus and is therefore potentially useful in screening for mutations in dominant disorders. HMA permits analysis of PCR products up to 1 kb in size; therefore, a 6-kb cDNA can be analysed with only six primer pairs, significantly fewer than would be required to screen the genomic sequence by SSCP. Initially, we screened a total of 10 individuals from four Alagille syndrome families, each with several affected members. None of these families demonstrated deletions of 20p12 by cytogenetic or molecular analysis. We used RT-PCR with six primer pairs generating overlapping cDNA fragments, A–F, sequentially covering most of the coding sequence (Fig. 6). Our goal was to localize the mutation within one of the six regions amplified, sequence the selected cDNA region to identify the mutation and then confirm the identified changes at the genomic level.

Family 1. HMA analysis indicated a mobility shift in the 'B' PCR product, which was seen in two affected individuals (Fig. 6*a*). Sequence analysis of *JAG1* cDNAs from affected members of this family demonstrated an 'AG' deletion at positions 1104 and 1105 (1104delAG). The deletion lies within exon 4, adjacent to the splice donor site.

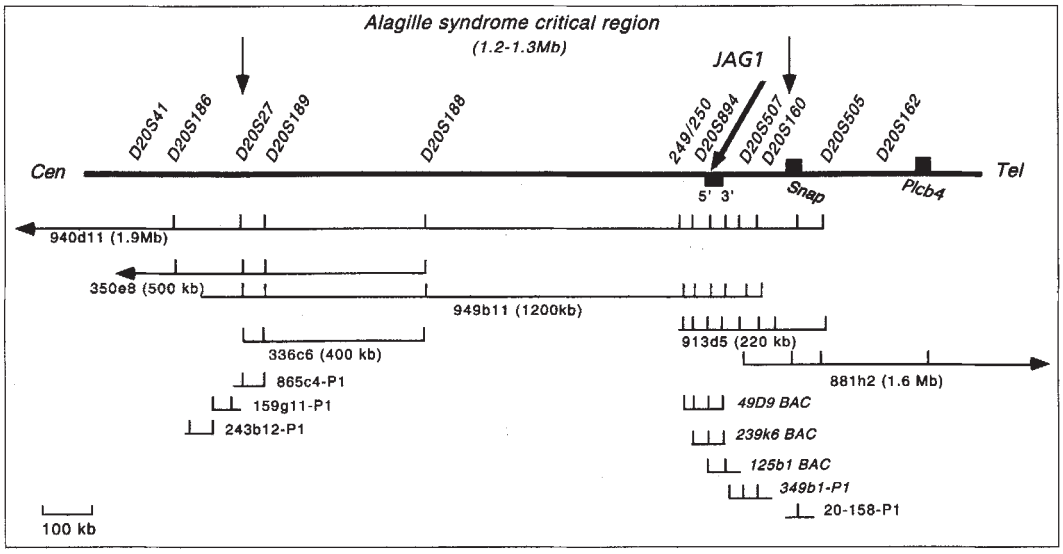

Fig. 3 Mapping *JAG1* to the Alagille syndrome-critical region. The critical region has been defined by the shortest region of overlap of patients with deletions of 20p12 by molecular and FISH mapping. It extends between P-1 243b12, proximal to *D20S27*, and clone 20 P1-158, proximal to *Snap*. YAC clones are indicated in standard print, P1 and BAC clones are indicated as such. BACs 49D9 and 125b1 were identified by screening a BAC library with primers from within the coding sequence of *JAG1*. STSs from within BAC 49D9 were used on a panel of clones from within the critical region to localize *JAG1* between *D20S894* and *D20S507*. Primers from within *JAG1* (exons 4, 23) localized to YACs 940d11, 949b11 and 913d5, and BACs 49D9, 125b1 and 239K6.

Table 2 • Mutations in *JAG1* in Alagille syndrome patients

Individuals	cDNA Mutations	Genomic DNA Mutations	Amino Acid Mutations		Predicted Translation Products
					SP DSL EGF-Repeats CR TM 1 1219
AGS Family 1	Deletion AG (1104-5)	Deletion AG Exon(n+2)	Amino Acid Change After 230	Normal: CN(230)RAICRQGCS Mutant: CN(230)SYLPTRLQS*	1 230 240(stop)
AGS Family 2	Insertion GTGGC (3102)	Insertion GTGGC Exon(n+21)	Amino Acid Change After 898	Normal: WCG(898)PRPCL... Mutant: WCG(898)VALDL...	1 898 945 (Stop)
AGS Family 3	Deletion CAGT (2531-34)	Deletion CAGT Exon(n+15)	Amino Acid Change After 708	Normal: DS(708)QCD... Mutant: DS(708)VMR...	1 708 741 (Stop)
AGS Family 4	Deletion C (2066)	Deletion C Exon(n+11)	Amino Acid Change After 553	Normal: FCKCP(553)ED... Mutant: FCKCP(553)RT...	1 553 563 (Stop)

Single-strand conformational polymorphism (SSCP) analysis of exon 4 on the extended family revealed a mobility shift in the three affected individuals (Fig. 6*a*). This deletion was confirmed by sequence analysis of the genomic DNAs of exon 4 (Fig. 6*a*). The 'AG' deletion leads to a reading frame shift at residue 230 (at the end of the DSL domain), resulting in a premature termination codon at residue 240 (deleting 979 residues of the protein) (Table 2).

The two affected brothers in this family have liver disease, heart disease (pulmonic and peripheral pulmonic stenosis), posterior embryotoxon and Alagille facies. Their less severely affected mother has a heart murmur, posterior embryotoxon and Alagille facies.

Family 2. On HMA, the PCR products from two affected members of AGS family 2 showed mobility shifts in the 'D' region (Fig. 6*b*). cDNA sequence analyses of amplified 'D' region sequences from both individuals revealed a five-nucleotide insertion (GTGGC) at position 3102 (3102ins5). The insertion is a repeat of the GTGGC sequence at position 3102 (exon 23) and found in all affected individuals of this family.

SSCP analysis revealed a novel band in this exon, which was present in an affected father and daughter but was not seen in the unaffected mother (Fig. 6*b*) or fifty matched normal controls (100 chromosomes). The insertion was confirmed by genomic sequence analysis of mutant *JAG1* in both affecteds. This insertion would cause a translational frameshift downstream of codon 898. Translation would be terminated at codon 945, generating JAG1 protein truncated by 274 residues. Thus, the mutant protein is predicted to contain the DSL domain, the entire EGF-like repeat domain, one third of the cysteine-rich (CR) domain and a segment of 47 residues altered by the translational frameshift. The remainder of the CR region, the transmembrane domain and the intracellular region would be deleted (Table 2).

In addition to the five-nucleotide insertion, cDNA sequence analysis of the amplified 'D' region revealed an 86-nucleotide deletion from positions 2785 to 2871. However, this variant was seen in all three members of the family (affected and unaffected) and corresponds to a complete absence of exon 20, suggesting that this product may result from alternative splicing of this exon. We observed a shift on heteroduplex analysis, consistent with the presence of variant cDNA in all ten individuals from the four families tested. RT-PCR experiments suggest that the ratio of species lacking exon 20 to those containing it is about 1:4 (data not shown). Loss of the 86-bp exon 20 would lead to a reading frame shift, producing a carboxyl-terminated truncated polypeptide that has lost the transmembrane domain. A similarly deleted *JAG1* cDNA has been observed in studies of human endothelial cells[34]. The significance of this altered product is not clear, and further experiments will determine whether there is a physiological role for this potentially soluble form of JAG1. The fact that this product is found in all individuals studied, and does not segregate with the Alagille syndrome phenotype, argues against a role in this disorder.

The phenotypes of the two affected members of family 2 are different from each other. The father demonstrates liver disease, cardiac disease and renal failure, while his daughter is more mildly affected with characteristic facies and pulmonary artery stenosis, although she has normal liver and kidney function to date.

Family 3. The two affected members of this family showed shifts in the 'C'-region PCR products on HMA analysis (Fig. 6*c*). Sequence analysis revealed a four-nucleotide deletion, 'CAGT', between bases 2531 and 2534 (exon 17) in both affected individuals (2531del4).

SSCP analysis of exon 17 revealed a novel band in the affected proband, in her affected mother and in the DNA from the concepticus of a terminated pregnancy (Fig. 6c). This SSCP variant was not identified in 50 ethnically matched controls (100 chromosomes). The four-nucleotide deletion was confirmed by genomic sequencing of exon 17 (Fig. 6*c*) from the affected indi-

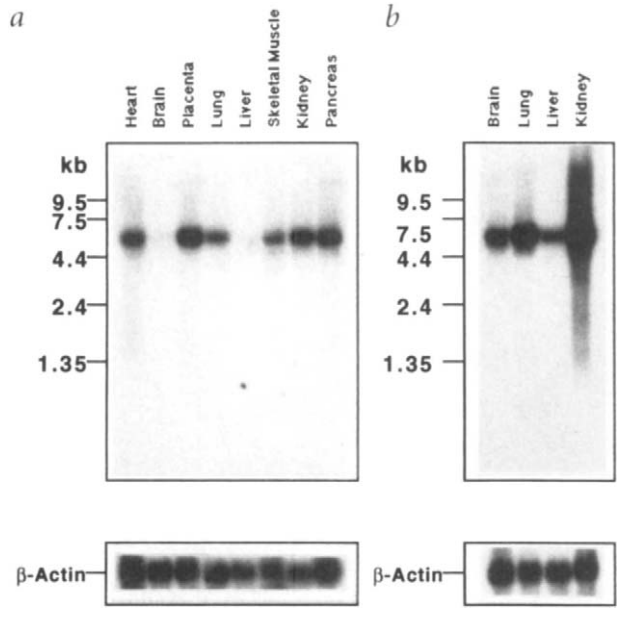

Fig. 4 Northern blot analysis of the *JAG1* expression in adult and fetal human tissues. A *JAG1* cDNA fragment and β-Actin cDNA were separately hybridized to the northern blots of both adult (***a***) and fetal (***b***) human tissues.

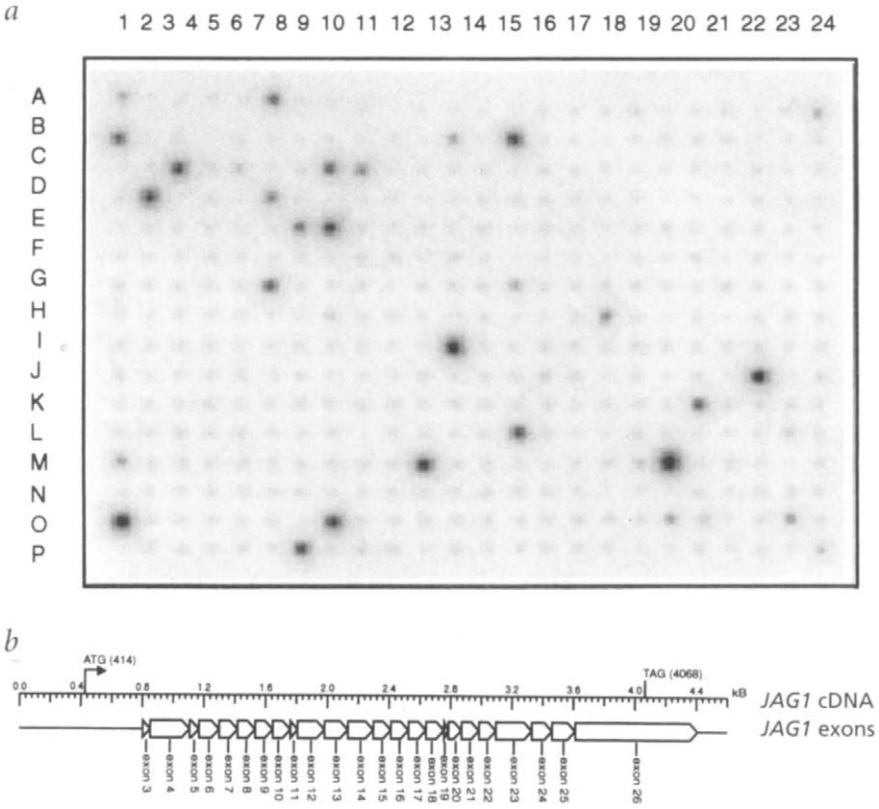

Fig. 5 Identification of the exon–intron boundary sequences of the *JAG1* gene by DNA array technology. ***a,*** Hybridization of *JAG1* cDNA to an array of sonicated BAC 49D9 DNA. The M13 single-strand fragments of BAC 49D9 DNA were arrayed on nylon membrane and hybridized with the full-length *JAG1* cDNA. ***b,*** Schematic diagram illustrating the alignment of the exon boundaries with the cDNA sequence of *JAG1*.

viduals. The mutant gene would encode a JAG1 protein that undergoes a translational frameshift at residue 741 with an altered segment of 33 amino acids before chain termination. The translational frameshift occurs in the twelfth EGF-like repeat (Table 2).

The proband in this family was severely affected, with liver involvement, severe branch pulmonary artery stenosis, butterfly vertebrae and a posterior embyrotoxon. She died at two and a half years of age from head trauma after a fall. Her mother has a milder phenotype, having come to medical attention at twenty years of age during pre-surgical evaluation for a basilar artery aneurysm. Studies at that time revealed abnormal liver function, and further workup revealed bile duct paucity, pulmonic stenosis, characteristic facies and posterior embryotoxon with retinal changes.

Family 4. No heteroduplexes were seen in any of the six PCR products from members of this family. However, cDNA sequence analysis revealed a single C nucleotide deletion at position 2066 in an affected daughter and father (2066delC) . This deletion lies in exon 13.

SSCP analysis of exon 13 reveals an altered band (Fig. 6*d*) in the proband and her father. Genomic sequence analyses verified the presence of the C deletion in exon 13 in both affected family members. This deletion would lead to a translational frameshift starting at residue 550 and an altered 13-residue segment before the protein chain terminates in the ninth EGF-like repeat (Table 2).

The proband was severely affected with liver and heart disease (tetralogy of Fallot), facial features, butterfly vertebrae and posterior embryotoxon. She died at five years of age from sepsis. Her father is mildly affected, with a history of a heart murmur and characteristic facies. The proband's sibling is also apparently affected, having severe congenital heart disease (tetralogy of Fallot) and posterior embryotoxon. Her liver function has been normal.

Discussion

We have localized *JAG1* within our previously defined Alagille-syndrome critical region on 20p12. We have found four distinct coding region mutations in this gene in four Alagille syndrome families, each with several affected members. The data presented here (and in the companion study[36]) suggest that mutations in *JAG1* cause the Alagille syndrome in that i) novel coding region mutations were identified and shown to segregate with disease phenotype in four families, ii) the mutations identified predict changes in function of JAG1 and iii) none of these changes were seen in 100 normal control chromosomes studied. In addition, the pattern of expression of *JAG1* is consistent with the phenotypic abnormalities seen in Alagille syndrome, as discussed below. We therefore conclude that the four distinct mutations in *JAG1* of patients with Alagille syndrome cause the disorder.

JAG1 is a ligand for the Notch receptor. Notch is a transmembrane protein with a large extracellular domain and a relatively short intracellular domain. The extracellular domain contains three conserved motifs: the DSL domain, 16 EGF-like repeats that mediate the interaction with Jagged and a cysteine-rich region. The activation of Notch by its ligand affects the expression of lineage-specific genes, leading to inhibition of differentiation along particular pathways. Thus, the overall effect of Notch activation is to restrict the number of cells that choose a specific cell fate, while leaving the cells poised to adopt alternative cell fates. For example, the activation of the Notch1 receptor by JAG1 inhibits granulocytic differentiation of 32D myeloid progenitor cells[12], and constitutively active Notch alters the balance of T cell subtypes in transgenic mice[23,24].

Notch and its ligands are broadly expressed in developing *Drosophila*, *C. elegans* and the rat. The relationship between expression and function is poorly understood. Expression studies of the *Jagged* genes in humans and other vertebrates reveal tissue patterns that are potentially consistent with the abnormalities seen in Alagille syndrome. *JAG1* is expressed in human fetal liver, heart and kidney as well as in the adult heart and kidney. We were unable to detect *JAG1* expression in adult liver, whereas expression in fetal liver at 16–32 weeks was detectable. The pathogenesis of bile duct paucity in Alagille syndrome is not known. Intralobular bile duct development and number is normal (or even increased) around the time of birth in a least some patients who eventually develop profound paucity later in infancy[38]. The bile ducts that are present are histologically and immunohistochemically normal. In addition, several groups have reported a reduction in the number of portal tracts in patients with Alagille syndrome[39], suggesting that the development of the portal tract or ductal plate may be abnormal. The Jagged–Notch interactions may be involved in the development of the portal tract itself and the bile ducts within it. As

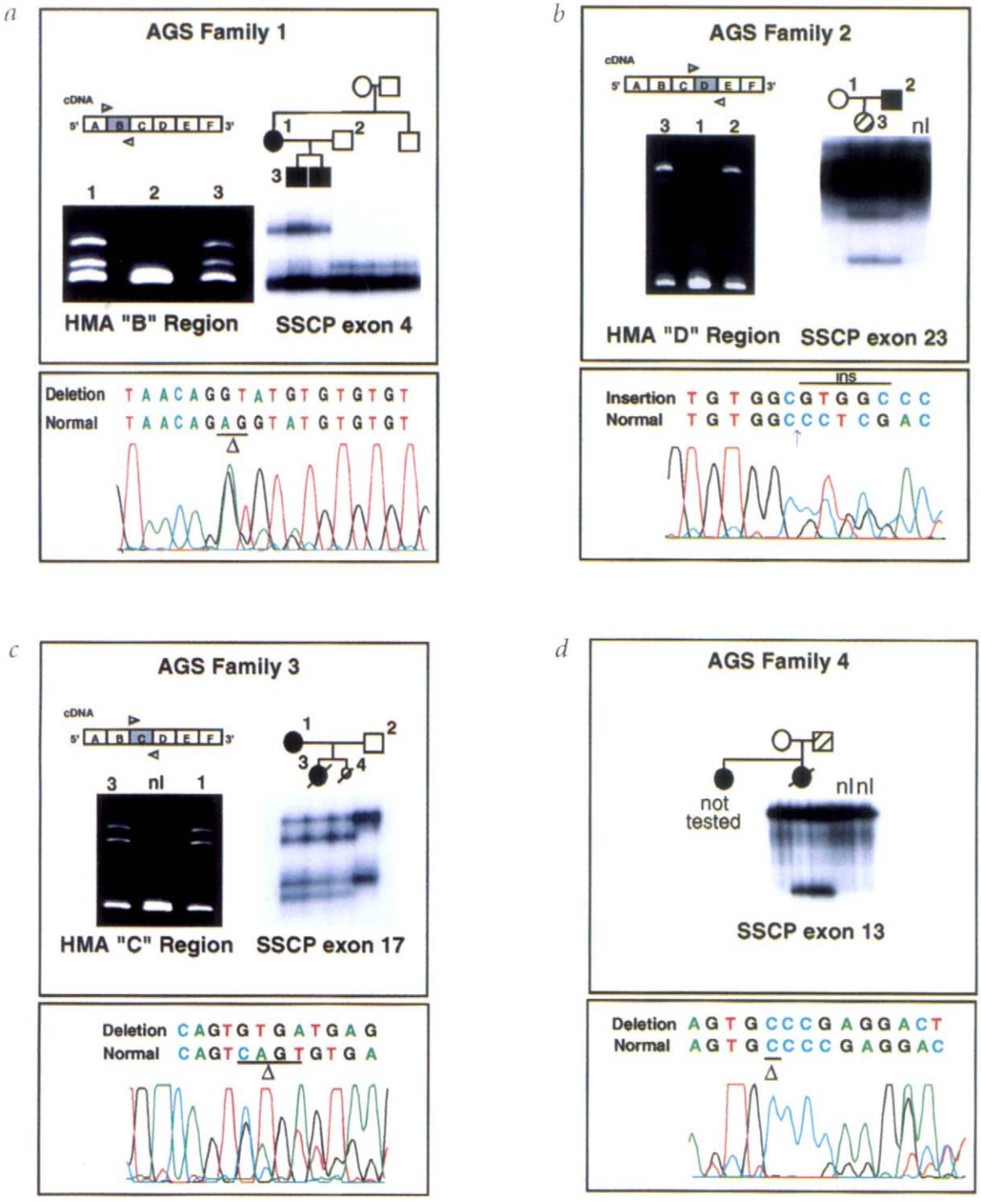

Fig. 6 HMA and SSCP analysis of *JAG1* in four families. Individuals with filled circles meet full criteria for diagnosis with Alagille syndrome. Individuals with hatched circles have some of the characteristics. ***a,*** HMA analysis in family 1 revealed a shift in the 'B' region of the cDNA in an affected mother and child. SSCP analysis of the extended pedigree revealed segregation of an exon 4 variant in two children and their mother. Sequence analysis demonstrates a 2-bp 'AG' deletion. ***b,*** HMA analysis demonstrates a heteroduplex shift in the 'D' region in an affected father and daughter. SSCP analysis confirmed segregation of an exon 23 variant. Sequence analysis reveals a 5-bp insertion (GTGGC) in father and daughter. ***c,*** The proband and mother from family 3 demonstrate an HMA band shift in the 'C' region. SSCP analysis revealed an exon 17 variant in an affected mother, her affected daughter and DNA from a terminated pregnancy. Sequence analysis reveals a 4-bp deletion in affected individuals. ***d,*** No band shifts were observed on heteroduplex analysis with the A, B, C, D, E or F primers in this family. SSCP analysis demonstrates an exon 13 variation in a child and her less severely affected father. A younger sibling has cardiac disease (tetralogy of Fallot), but has not been tested. Sequence analysis in father and daughter demonstrated a single nucleotide 'C' deletion. nl, normal individual demonstrating wild-type pattern.

approximately one-third of Alagille syndrome patients have renal dysfunction[4], the expression of the Jagged protein in the kidney is indicative of its role in normal renal development.

The expression of the *rJagged* gene throughout the nervous system of the rat[40] is interesting in that neurologic abnormalities are not a prominent feature in Alagille syndrome. In earlier reports, mental retardation was mentioned as a significant feature of the syndrome[1], but this may have been secondary to the severe nutri-

tional debilitation arising from liver and cardiac disease. We did not find developmental delay or mental retardation to be a significant feature, perhaps reflecting earlier diagnosis and improved nutritional support[4] . By contrast, the expression of *rJagged1* in the rat eye and first branchial cleft is consistent with *JAG1* mutations potentially resulting in the ocular and facial abnormalities seen in Alagille syndrome.

Studies of a homozygous Notch1 mutant in mouse demonstrate that formation of the somites is abnormal in the absence of Notch1, suggesting a role for this pathway in somite development[41]. Abnormal somite formation is also a consequence of homozygous mutations of the mouse *Delta* homologue[42]. Abnormalities in somite development may be responsible for the vertebral defects associated with Alagille syndrome and may contribute to the facial features as well.

The *Notch* genes themselves have been implicated in human disease in two other instances. A T-cell leukaemia has been shown to be caused by a t(7;9) chromosomal translocation that interrupts the *Notch1 (TAN1)* locus at 9q34 (ref. 27). Germ-line mutations in *Notch3* have been found in patients with a disorder termed CADASIL (cerebral autosomal dominant arteriopathy with subcortical infarcts and leukoencephalopathy). CADASIL is a disease with onset during the fifth decade that is characterized by stroke and dementia, and is associated with diffuse white-matter abnormalities on neuro-imaging[43].

The dominant inheritance demonstrated in Alagille syndrome is consistent with our observation that all affected individuals had wild-type as well as mutant *JAG1* alleles. All the mutations in *JAG1* that we have identified result in translational frameshifts, which would be expected to cause significant disruption of the protein and its function. The mutations were all localized within the conserved regions of JAG1, in the DSL domain, within the EGF-like repeats or in the CR region. Previously, we studied several patients with sizable deletions encompassing the entire *JAG1* gene, and these patients have phenotypes that are similar to those seen in patients with intragenic mutations[4,9,10]. In these patients, the normal allele does not rescue the phenotype caused by the absent protein, indicating that Alagille syndrome is caused by haploinsufficiency of *JAG1*. In patients with a mutant rather than an absent *JAG1* allele, the disease can be caused either by haploinsufficiency of the normal product or by a dominant negative effect of the mutant protein. Further studies are needed to distinguish between these alternative mechanisms.

Cytogenetically detectable deletions for most regions of the human genome are associated with phenotypic abnormalities, presumably caused by haploinsufficiency of the various genes involved. Less is known about the phenotypic effects of haploinsufficiency for single genes, although there are some well documented examples. Genes for which haploinsufficiency causes disease either code for proteins that are required in large amounts, with monosomy leading to insufficient product, or code for regulatory molecules whose concentration is closely titrated within the organism[44]. Dominant human diseases associated with haploinsufficiency include Williams syndrome[45] (deletion of the elastin gene and possibly other genes) and Rubinstein-Taybi syndrome[46] (deletion or mutation of the gene encoding the CREB-binding protein).

Data from *Drosophila* are consistent with a haploinsufficient phenotype for genes of the Notch signaling pathway as well. Both *Delta*- and *Notch*-deficient heterozygotes demonstrate mutant phenotypes[47]. Additionally, when mosaic flies were studied with cells carrying one, two or three copies of a wild-type *Notch* allele, variations were observed in cell fate choices that correlated with the number of copies of *Notch*[48]. These results indicate that slight variations in the concentration of gene products in this pathway can have phenotypic effects.

Our data suggest that there are other factors (genetic or environmental) that modify the effects of *JAG1* mutations on phenotype. In each of the families we have studied, the segregating mutations are associated with highly variable phenotypic expression. For example, in AGS family 4, phenotypes range from subclinical (father with facial characteristics and clinically insignificant heart murmur) to severe (child with severe heart and liver disease).

In this report, we have shown that mutations in *JAG1*, encoding a Notch-ligand, cause Alagille syndrome, a developmental disorder in humans. The expression pattern of *JAG1* and the cellular mechanism of action of the Notch signaling pathway provide insight into the pathogenesis of the multi-system involvement seen in Alagille syndrome.

Methods

Alagille syndrome patients. Patients studied had undergone a full diagnostic workup for Alagille syndrome and all probands met the diagnostic criteria for the disorder. The proband of each family had Alagille syndrome as judged from the presence of bile duct paucity in addition to a minimum of three of five clinical criteria (cholestasis, cardiac disease, vertebral anomalies, anterior chamber defects of the eye, characteristic facial features). Additional family members were examined by a member of our group, or medical records were requested and reviewed. All patients and their families were enrolled in the study under an IRB-approved protocol at the Children's Hospital of Philadelphia.

Physical mapping. CEPH human YAC clones were identified through the Whitehead Institute for Biomedical Research/MIT Center for Genomic Research web site and published data[49] and provided by M. Budarf at the Children's Hospital of Philadelphia. The human P1 library[50] was screened as previously described[53]. The human BAC library[52,53] was screened according to the protocol supplied by Research Genetics. Selected clones were mapped by FISH and STS content analysis to confirm cytogenetic localization and order the clones. When clones were not contiguous, clone ends were obtained by sequencing with T7 and SP6 promoters, and new PCR primers were designed for the next round of library screening. Sequencing was carried out in the Nucleic Acid Sequencing Cores at the University of Pennsylvania (Department of Genetics) and at the Children's Hospital of Philadelphia. Fluorescence *in situ* hybridization studies were carried out by standard techniques as previously described[4,45].

Northern blot analysis. Northern blots (Clontech) of multiple human tissues and human fetal tissues were hybridized with a 400-bp fragment of *JAG1* cDNA (amplified by the PCR with primer pair 292, AGATCCTGTCCATGCAGAACGT, and 293, ATACTCAAAGTG GGCAACGCC). QuikHyb hybridization solution (Stratagene) was used for both prehybridizations and hybridizations, which were performed at 60 °C. ^{32}P-probes denatured by boiling), together with salmon sperm DNA (100 µg/15 ml), were directly added to the prehybridization solution for hybridization. Membranes were washed twice in 2× SSC/0.1% SDS at room temperature for 10 min, then once in 0.1× SSC/0.1% SDS at 60 °C for 20 min. *β-Actin* cDNA (ClonTech) was used as a control probe for northern blots.

DNA array. A BAC clone containing the *JAG1* gene locus (49D9) was sonicated to break it into small fragments. DNA fragments of 1.5 to 2.0 kb were selected and ligated into an M13 vector. Single-stranded M13 clones were arrayed onto four duplicate nylon membranes with a 384-pin replicator (Schummer, M. *et al.*, manuscript submitted). This array was hybridized with the full-length *JAG1* cDNA. Positive M13 clones were picked and sequenced with the M13 forward primer. Analysis of the reverse sequence was performed on the PCR amplified double-strand M13 DNA with –21M13 primer (ABI). The exon–intron boundary sequences were identified by alignment of the genomic sequence with the *JAG1* cDNA sequence.

Oligonucleotides. All primers are indicated in the 5'→3' direction. Primers for RT-PCR segments of the *JAG-1* cDNA—including A, B, C, D, E and F—were amplified, respectively, with primer pairs 292/395 (AGATCCTGTCCATGCAGA ACGT/CATCCAGCCTTCCATGCAA), 398/399 (CTTTGAGTATCAGATCCGCGTGA/ CGATGTCCAGCTGACAGA), 402/403 (CGGGATTTGGTTAATGGTTAT/GGTACCAGTTGTCTCCAT),

406/407 (GGAACAACCTGTAACATAGC/GGCCACATGTATT TCATTGTT), 408/409 (GAATATTCAATCTACATCGCTT/CTCAGACTCGAGTA TGACACGA) and 410/411 (AAAGTGCCCAGAGCTTAAACCG/GGTGTTTTAAACATCTGACGTCGTA. Primers for exons 4, 13, 17 and 23 were amplified, respectively, with primer pairs 510/511 (CAGGGAAGAAGGCTGCAATGT/TGGTGGGGTGATAAATGGACAC), 447/448 (GTTTTACTCTGATCCCTC/CAAGGGGCAGTGGTAGTAAGT), 455/456 (GCTATCTCTGGGACCCTT/CCACGTGGGGCATAAAGTT) and 467/468 (ATGGCTGCCGCAGTTCA/CAAGCAGACATCCACCAT). Microsatellite markers: (TTTG)n amplified with primer pair 249/250 (GGTCTTTTGCCACTGTTT/GAATAGGGAGGAGAAAAC). (GTTT)n amplified with primer pair 247/248 (GTCTTTTGCCACTGTTTG/GAA TAGGGAGGAGAAAAC).

Sequence analysis. Procedures used for DNA sequence were previously described[54]. Briefly, the BAC DNA was sequenced with a random shotgun sequencing approach. A shotgun library was constructed by sonicating plasmid DNA, size-selecting 1.5–2-kb fragments on an agarose gel, blunting the ends of the fragments with mung bean nuclease and cloning the fragments into *Sma*I–digested M13-mp18 vector (Novagen). Single-strand DNA was prepared from single plaques. Approximately 100 single-strand DNA templates were sequenced. cDNA fragments were cloned into pCR.2.1 vector (TA cloning system, Invitrogen), prepared using 5'-3' DNA mini-preparation system (5'prime-3'prime, Inc.) and sequenced. Fluorescently labelled –21M13 primer was used for sequencing of single-strand DNA and fluorescently labelled –21M13 and M13 forward primers were used for double-strand cDNA following the manufacture's procedure (ABI).

RT-PCR and heteroduplex mobility analysis. Total RNA was isolated with a Trizol RNA isolation kit (GIBCO-BRL). cDNA was synthesized with a reverse transcription system following the manufacture's procedure (GIBCO BRL). One twentieth the volume of the reverse-transcribed cDNA was amplified with Taq polymerase (Perkin Elmer). Heteroduplex mobility analysis was performed as follows: 200–500 ng of DNA was denatured at 96 °C for 5 min in a denaturing buffer [0.1M NaCl, 10mM Tris.HCl (pH 7.8) and 2mM EDTA], immediately removed to a wet ice bath for 5 min and then incubated at 55 °C for 5 min. The re-annealed DNA was mixed with loading buffer (0.2% Orange G, 2.5% Ficoll) and then electrophoresed on a 5% polyacrylamide gel (19.5×19 cm) in 1× TBE buffer for 3–3.5 h at 250 volts. After electrophoresis, the gel was stained in 0.5 μg/ml ethidium bromide.

SSCP. DNA was extracted from lymphocytes (whole blood) or established lymphoblastoid cell lines of affected and unaffected members of each Alagille family and from unrelated normal control subjects with the Puregene DNA isolation kit (Gentra Systems, Inc.). The primers for PCR analysis were designed to cover all exons as well as the intron–exon boundaries of *JAG1* as outlined in Table 1. For SSCP analysis, each PCR reaction contained (in a final volume of 25 μl) 75 ng of genomic DNA, 200 μM dATP, dTTP and dGTP, and 62.5 μM dCTP, 4 μCi of ^{32}P dCTP, 10 pM of each primer, 1.0–1.5 mM $MgCl_2$, 2.5 μl of dimethyl sulfoxide, 2.5 ul of 10×PCR Buffer II (Perkin Elmer) and 0.75 U AmpliTaq polymerase (Perkin Elmer). PCR conditions were as follows: 94 °C, 30 s; 50 °C, 1 min; 72 °C, 30 s for 35 cycles. For SSCP analysis, the denatured PCR products were electrophoresed on MDE gels (FMC) with and without glycerol at 4 °C for 4–5 h. Gels were transferred to filter paper and exposed to X-ray film at –70 °C for 1–24 h. Amplicons demonstrating SSCP band shifts were sequenced by the Nucleic Acid/Protein Core facility of the Children's Hospital of Philadelphia with an ABI 373A automated sequencer.

GenBank accession Nos. *JAG1* cDNA U73936 (on which the numbering system in this paper is based), U61276.

Acknowledgements

We thank T. Kadesch for discussion and critique of the manuscript and X. He and J. Mullins for training in HMA analysis. We would also like to thank R. Oakey, P. Chaudhary, M.Budarf, P. Nelson, M. Bucan, I. Hansmann, E. Roessler, and C. Witzleben for helpful discussions and B. Emanuel for critical reading of the manuscript. We are grateful to R. Baumgarner, D. Baskin, J. Faust, C. Loretz, Z. Wang and E. Rapaport for DNA sequencing and figure preparation. M. Schummer and W. Ng assisted with DNA array technology. We thank the families of Alagille syndrome patients and the Alagille syndrome Alliance for their encouragement and support. We are grateful to S. Peck, M. Huggins and the residents and fellows who care for the patients. We thank M. Muenke and K. Ohene-Frempong for control DNA samples. This work was supported by Clinical Research Grant No. FY-96-0682/FY-97-0565 from the March of Dimes Birth Defects Foundation (NBS), NIH grant 1R01DK53104-01 (NBS), Fight for Sight grant GA96046 (NBS), a MAPS scholar award supported by NIH grant 5 P30 HD288215 (IDK), DK02338-03 (EBR), and a Michael Geisman research fellowship and Children's Brittle Bone Foundation (MQ). L. Li is supported by the Stowers Institute for Medical Research. Physical mapping described in this manuscript was supported in part by USPHS Grant CA 58207, the U.S. Department of Energy under contract DE-AC-03-76SF00098 and Vysis, Inc.

Received 6 May; accepted 6 June 1997.

1. Alagille, D. *et al.* Syndromic paucity of interlobular bile ducts. *J. Pediatr.* **110,** 195–200 (1987).
2. Krantz, I.D., Piccoli, D.A. & Spinner, N.B. Alagille syndrome. *J. Med. Genet.* **34,** 152–157 (1997).
3. Danks, D.M., Campbell, P.E., Jack, I., Rogers, J. & Smith, A.L. Studies of the aetiology of neonatal hepatitis and biliary atresia. *Arch. Dis. Child* **52,** 360–367 (1977).
4. Krantz, I.D. *et al.* Deletions of 20p12 in Alagille syndrome: frequency and molecular characterization. *Am. J. Med. Genet.* **70,** 80–86 (1997).
5. Piccoli, D.A. & Witzleben, C.L. Disorders of the intrahepatic bile ducts. in *Gastrointestinal disease: pathophysiology, Diagnosis, Management,* 3rd ed (eds Walker, D.A. *et al.)* 1124–1140 (B.C. Decker, Philadelphia, 1991).
6. Watson G.H. & Miller, V. Arteriohepatic dysplasia: familial pulmonary arterial stenosis with neonatal liver disease. *Arch. Dis. Child.* **48,** 459–466 (1973).
7. Dhorne-Pollet, S., Deleuze, J.-F., Hadchouel, M. & Bonaiti-Pellie, C. Segregation analysis of Alagille syndrome. *J. Med. Genet.* **31,** 453–457 (1994).
8. Schnittger, S., Hofers, C., Heidemann, P., Beermann, F. & Hansmann, I. Molecular and cytogenetic analysis of an interstitial 20p deletion associated with syndromic intrahepatic ductular hypoplasia (Alagille syndrome). *Hum. Genet.* **83,** 239–244 (1989).
9. Spinner N.B. *et al.* Cytologically balanced t(2;20) in a two generation family with Alagille syndrome: cytogenetic and molecular studies. *Am. J. Hum. Genet.* **55,** 238–243 (1994).
10. Rand, E.B., Spinner, N.B., Piccoli, D.A., Whitington, P.F. & Taub, R. Molecular analysis of 24 Alagille syndrome families identifies a single submicroscopic deletion and further localizes the Alagille region within 20p12. *Am. J. Hum. Genet.* **57,** 1068–1073 (1995).
11. Deleuze, J.-F., Hazan J., Dhorne S., Weissenbach, J. & Hadchouel, M. Mapping of microsatellite markers in the Alagille region and screening of microdeletions by genotyping 23 patients. *Eur. J. Hum. Genet.* 2, 185–190 (1994).
12. Li, L. *et al.* Human homolog of rat Jagged, *JAG1*, inhibits granulocytic differentiation of 32D myeloid progenitors through interaction with Notch1. *Immunity* (in press).
13. Greenwald, I. & Rubin, G. M. Making a difference: the role of cell-cell interactions in establishing separate identities for equivalent cells. *Cell* **68,** 271–281 (1992).
14. Fortini, M.E., Rebay, I., Caron, L.A. & Artavanis-Tsakonas, S. An activated Notch receptor blocks cell-fate commitment in the developing *Drosophila* eye. *Nature* **365,** 555–557 (1993).
15. Artavanis-Tsakonas, S., Matsuno, K. & Fortini, M.E. Notch signaling. *Science* **268,** 225–232 (1995).
16. Franco del Amo, F. *et al.* Expression pattern of Motch, a mouse homolog of *Drosophila* Notch, suggests an important role in early postimplantation mouse development. *Development* **115,** 737–744 (1992).
17. Reaume, A.G., Conlon, R. A., Zirngibl, R., Yamaguchi, T. P & Rossant, J. Expression analysis of a Notch homologue in the mouse embryo. *Dev. Biol.* **154,** 377–387 (1992).
18. Kopan, R. & Weintraub, H. Mouse Notch: expression in hair follicles correlates with cell fate determination. *J. Cell Biol.* **121,** 631–641 (1993).
19. Lardeli, M., Dahlstrand, J. & Lendahl, U. The novel Notch homolog mouse Notch3 lacks specific epidermal growth factor-repeats and is expressed in proliferating neuroepithelium. *Mech. Dev.* **46,** 123–136 (1994).
20. Weinmaster, G., Roberts, V. J. & Lemke, G. A homolog of *Drosophila* Notch expressed during mammalian development. *Development* **113,** 199–205 (1991).
21. Weinmaster, G., Roberts, V.J. & Lemke, G. Notch2: a second mammalian Notch gene. *Development* **116,** 931–941 (1992).
22. Uyttendaele, H. *et al.* Notch4/int-3, a mammary proto-oncogene, is an endothelial cell-specific mammalian Notch gene. *Development* **122,** 2251–2259 (1996).
23. Robey, E. *et al.* An activated form of Notch influences the choice between CD4 and CD8 T cell lineages. *Cell* **87,** 483–492 (1996).
24. Washburn, T. *et al.* Notch activity influences the αβ versus γδ T cell lineage decision. *Cell* **88,** 833–843 (1997).
25. Swiatek, P.J., Lindsell, C.E., del Amo, F., Weinmaster, G. & Gridley, T. Notch1 is essential for postimplantation development in mice. *Genes Dev.* **8,** 707–719 (1994).
26. Bao, Z.Z. & Cepko, C.L. The expression and function of Notch pathway genes in the developing rat eye. *J. Neurosci.* **17,** 1425–1434.
27. Ellisen, L.W. *et al.* TAN-1, the human homolog of the *Drosophila* Notch gene, is broken by chromosomal translocations in T lymphoblastic neoplasms. *Cell* 66, 649–661 (1991).
28. Sugaya, K. *et al.* Three genes in the human MHC class III region near the junction

with the class II: gene for receptor of advanced glycosylation end products, PBX2 homeobox gene and a Notch homolog, human counterpart of mouse mammary tumor gene *int-3*. *Genomics* 23, 408–419 (1994).
29. Muskavitch, M.A. & Hoffman, F.M. Homologs of vertebrate growth factors in *Drosophila melanogaster* and other vertebrates. *Curr. Topics Dev. Biol.* **24,** 289–328 (1990).
30. Lindsell, C.E., Shawber, C.J., Boulter, J. & Weinmaster, G. Jagged: a mammalian ligand that activates Notch1. *Cell* **80,** 909–917 (1995).
31. Henderson, S.T., Gao, D., Lambie, E. J. & Kimble, J. Lag-2 may encode a signaling ligand for the GLP-1 and LIN-12 receptors of *C. elegans*. *Development* **120,** 2913–2924 (1994).
32. Lieber, T. *et al.* Single amino acid substitutions in EGF-like elements of Notch and Delta modify *Drosophila* development and affect cell adhesion *in vitro*. *Neuron* **9,** 847–859 (1992).
33. Shawber, C.J., Boulter, J., Lindsell, C. E. & Weinmaster, G. Jagged2: A Serrate-like gene expressed during rat embryogenesis. *Dev. Biol.* **180,** 370–376 (1996).
34. Zimrin A.B. *et al.* An antisense oligonucleotide to the Notch ligand Jagged enhances fibroblast growth factor-induced angiogenesis in vitro. *J. Biol. Chem.* **51,** 32499–32502 (1996).
35. Spinner, N.B. *et al.* Mapping the Alagille syndrome critical region within 20p12. Proc. Single Chromosome 20 Workshop, February 1997, Hinxton, Cambridgeshire, UK *Cytogenetic. Cell Genet.* (in press).
36. Oda, T. *et al.* Mutations in the human Jagged1 Gene (JAGL1) are responsible for the Alagille syndrome. *Nat. Genet.* **16,** 235–242 (1997).
37. Delwart, E.L. *et al.* Genetic relationships determined by a DNA heteroduplex mobility assay: analysis of HIV-1 env genes. *Science* **262,** 1257–1261 (1993).
38. Kahn E. *et al.* Nonsyndromic paucity of interlobular bile ducts: light and electron microscopic evaluation of sequential liver biopsies in early childhood. *Hepatology* **6,** 890–901 (1986) .
39. Novotny, N.M., Zetterman, R.K., Antonson D.L. & Vanderhoof J.A. Variation in liver histology in Alagille's syndrome. *Am. J. Gastroenterol.* **75,** 449–506 (1981).
40. Lindsell, C.E., Boulter, J., diSibio, G., Gossler, A. & Weinmaster G. Expression patterns of Jagged, Delta1, Notch1, Notch2, and Notch3 genes identify ligand-receptor pairs that may function in neural development. *Mol. Cell. Neurosci.* **8,**14–27 (1996).
41. Conlon, R.A., Reaume, A.G. & Rossant, J. Notch1 is required for the coordinate segmentation of somites. *Development* **121,**1533–1545 (1995).
42. de Angeles, M.H., McIntyre, J., II & Gossler, A. Maintenance of somite borders in mice requires the Delta homologue Dll1. *Nature* **386,** 717–721 (1997).
43. Joutel, A. *et al.* Notch3 mutations in CADASIL, a hereditary adult-onset condition causing stroke and dementia. *Nature* **383,**707–710 (1996).
44. Wilkie, A.O.M. The molecular basis of genetic dominance. *J. Med. Genet.* **31,** 89–98
45. Nickerson, E., Greenberg, F., Keating M.T., McCaskill C. & Shaffer, L.G. Deletions of the elastin gene at 7q11.23 occur in ~90% of patients with Williams syndrome. *Am. J. Hum. Genet.* **56,**1156–1161 (1995).
46. Petrij, F. *et al.* Rubinstein-Taybi syndrome caused by mutations in the transcriptional co-activator CBP. *Nature* **376,** 348–351 (1995).
47. Lindsley, D.L. & Zimm G.G. The genome of *Drosophila melanogaster* (Academic Press, New York, 1992).
48. Heitzler, P. & Simpson, P. The choice of cell fate in the epidermis of *Drosophila*. *Cell* **64,** 1083–1092 (1991).
49. Pollet, N *et al.* Construction of a 3.7 Mb physical map within human chromosome 20p12 ordering 18 markers in the Alagille syndrome locus. *Genomics* **27,** 467–474 (1995).
50. Shepherd, N.S. *et al.* Preparation and screening of an arrayed human genomic library generated with the P1 cloning system. *Proc. Natl. Acad. Sci USA* **91,** 2629–2633 (1994).
51. Stokke, T. *et al.* A physical map of chromosome 20 established using fluorescence in situ hybridization and digital image analysis. *Genomics* **26,** 134–137 (1995).
52. Shizuya, H. *et al.* Cloning and stable maintenance of 300-kilobase-pair fragments of human DNA in *Escherichia coli* using an F-factor based vector. *Proc. Natl. Acad. Sci USA* **89,** 8794–8797 (1992).
53. Kim, U.-J. *et al.* Construction and characterization of a human bacterial artificial chromosome library. *Genomics* **34,** 213–218 (1996).
54. Smith, T.M. *et al.* Complete genomic sequence and analysis of 117 kb of human DNA containing the gene BRCA1. *Genome Res.* **6,** 1029–1049 (1996).